Metal-Insulator Transition and Orbital Order in $PbRuO_3$

Simon A. J. Kimber,[1,2] Jennifer A. Rodgers,[2] Hua Wu,[3] Claire A. Murray,[2] Dimitri N. Argyriou,[1] Andrew N. Fitch,[4] Daniel I. Khomskii,[3,5] and J. Paul Attfield[2,*]

[1]*Helmholtz-Zentrum Berlin für Materialien und Energie, 100 Glienicker Straße, 14109 Berlin, Germany*
[2]*Centre for Science at Extreme Conditions and School of Chemistry, University of Edinburgh, King's Buildings, Mayfield Road, Edinburgh EH9 3JZ, United Kingdom*
[3]*II. Physikalisches Institut, Universität zu Köln, Zülpicher Straße 77, D-50937 Köln, Germany*
[4]*European Synchrotron Radiation Facility, B.P. 220, 38043 Grenoble Cedex, France*
[5]*Department of Physics, Loughborough University, Leicestershire LE11 3TU, United Kingdom*
(Received 20 November 2008; published 29 January 2009)

Anomalous low temperature electronic and structural behavior has been discovered in $PbRuO_3$. The structure [space group *Pnma*, $a = 5.563\,14(1)$, $b = 7.864\,68(1)$, $c = 5.614\,30(1)$ Å] and metallic conductivity at 290 K are similar to those of $SrRuO_3$ and other ruthenate perovskites, but a sharp metal-insulator transition at which the resistivity increases by 4 orders of magnitude is discovered at 90 K. This is accompanied by a first-order structural transition to an *Imma* phase [$a = 5.569\,62(1)$, $b = 7.745\,50(1)$, $c = 5.662\,08(1)$ Å at 25 K] that shows a coupling of Ru^{4+} $4d$ orbital order to distortions from Pb^{2+} $6s6p$ orbital hybridization. The *Pnma* to *Imma* transition is an unconventional reversal of the group-subgroup symmetry relationship. No long range magnetic order is evident down to 1.5 K. Calculations show that Pb $6s6p$ and Ru $4d$ orbital hybridization and strong spin-orbit coupling are significant.

DOI: 10.1103/PhysRevLett.102.046409 PACS numbers: 71.30.+h, 61.66.Fn, 71.20.Ps

Transition metal oxide perovskites display a remarkable range of electronic phenomena such as superconductivity, colossal magnetoresistances, and coupled charge, orbital, and spin orderings [1]. Perovskite-related ruthenates based on Ru^{4+} have proved interesting as broad Ru : $4d$ bands lead to metallicity without chemical doping, so very clean correlated itinerant electron physics may be observed in single crystals. The layered perovskite Sr_2RuO_4 is a p-wave superconductor [2], while bilayered $Sr_3Ru_2O_7$ is a metallic metamagnet [3]. All of the cubic-type $ARuO_3$ perovskites (A = Ca, Sr, Ba) are metallic to the lowest measured temperatures. $SrRuO_3$ and $BaRuO_3$ are ferromagnets with Curie temperatures of $T_C = 160$ and 60 K, respectively [4–7], but $CaRuO_3$ does not show a magnetic transition [8]. Another ruthenate perovskite, $PbRuO_3$, was synthesized at high pressures in 1970 [9], but the electronic properties of this material have not been reported. Pb^{2+} is intermediate in size between Sr^{2+} and Ba^{2+}, so $PbRuO_3$ is expected to be a ferromagnetic metal. However, in this Letter, we report that $PbRuO_3$ behaves very differently from the other $ARuO_3$ perovskites and instead shows a sharp metal-insulator transition at 90 K but without apparent long range spin order. Electron localization is strongly coupled to the lattice through Ru-orbital ordering, resulting in an anomalous structural change to higher lattice symmetry at low temperatures. We propose that strong hybridization of Ru $4d$ with Pb $6s$ and $6p$ states and spin-orbit coupling are responsible for inducing this alternative ground state for ruthenate perovskites.

Small (ca. 10 mg) polycrystalline pellets of $PbRuO_3$ were synthesized by heating the oxygen-deficient pyrochlore $Pb_2Ru_2O_{6.5}$ at 11 GPa and 1100 °C using a Walker-type multianvil press. Synchrotron x-ray diffraction profiles in the temperature range $10 < T < 300$ K were collected from instrument ID31 at the ESRF, France, with wavelength $\lambda = 0.45\,621$ Å, and time-of-flight neutron powder data were recorded using the GEM spectrometer at ISIS, United Kingdom, over the range $1.5 < T < 300$ K. Rietveld fits to diffraction data were performed using the GSAS package [10]. Magnetic susceptibility and electronic resistivity measurements were made using Quantum Design MPMS and PPMS (Magnetic and Physical Properties Measurement System) instruments.

The (hkl) Bragg reflections observed in the room temperature x-ray and neutron powder diffraction profiles of $PbRuO_3$ are all consistent with the orthorhombic *Pnma* space group of $SrRuO_3$ [11], and refinement of this model gave good fits to the data. We also attempted refinements of noncentrosymmetric variants of this structure, in case of a steric (''lone pair'') effect from the Pb $6s^2$ state, but no improvements were obtained and the fits diverged. All of the site occupancies refined to within error (ca. 1%) of full occupancy, showing that the sample is stoichiometric [12]. The *Pnma* superstructure is often observed in oxide perovskites and results from a generic, oxygen-centered, tilting instability rather than specific, transition metal-centered electronic instabilities.

To compare the contributions of Pb^{2+} and Sr^{2+} to the ruthenate band structures, we performed electronic structure calculations for room temperature *Pnma*-type $PbRuO_3$ and $SrRuO_3$ [13] in the local density approximation (LDA) using the full-potential augmented plane wave plus local orbital method [14]. The results (Fig. 1) for $SrRuO_3$ are very similar to those previously reported [5].

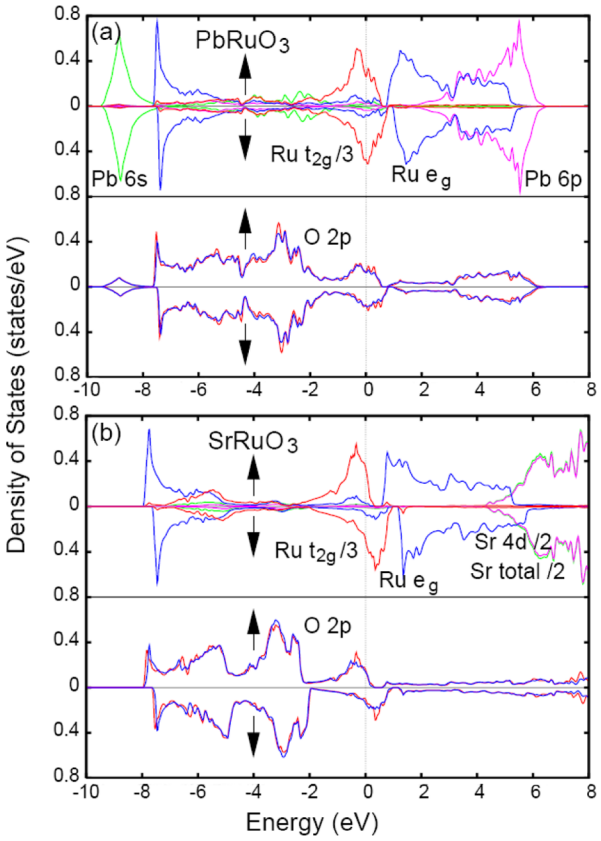

FIG. 1 (color online). Density of states (DOS) of (a) $PbRuO_3$ and (b) $SrRuO_3$ in the *Pnma* structure calculated by the LDA in the ferromagnetic state. Up (down) arrows refers to spin up (down). The Ru t_{2g} DOS is scaled by $\frac{1}{3}$, and the Sr DOS is scaled by $\frac{1}{2}$. The exchange splitting of the Ru t_{2g}-O $2p$ bands is significantly suppressed in $PbRuO_3$.

The Sr^{2+} states lie far from the Ru $4d$-O $2p$ bands near the Fermi level [6], and a large exchange splitting is found. The itinerant ferromagnetic state is stabilized by 25 meV/f.u., in keeping with the 160 K Curie transition. By contrast, the Ru $4d$ and O $2p$ states in $PbRuO_3$ lie just between the occupied Pb $6s$ and unoccupied Pb $6p$ states. The Ru t_{2g}-Pb $6s$ and Ru e_g- Pb $6p$ hybridizations, both aided by the O $2p$ state, and t_{2g}-e_g mixing due to the lattice distortion, significantly suppress the exchange splitting of the Ru t_{2g}-O $2p$ conduction bands, reducing the magnetic stabilization energy to near zero (<4 meV/f.u.). To confirm that the slight lattice differences between the two materials are unimportant, we also calculated the electronic structure of $SrRuO_3$ using the $PbRuO_3$ parameters and found that the electronic and magnetic properties were virtually identical.

An unexpected difference between $PbRuO_3$ and the other perovskite ruthenates was discovered by resistivity measurements (Fig. 2). At ambient temperatures, the $PbRuO_3$ has a resistivity of $\sim 10^{-1}$ Ω cm with little temperature dependence, characteristic of metallic conduction with a resistive grain boundary contribution. However, on cooling, the resistivity increases sharply by 4 orders of

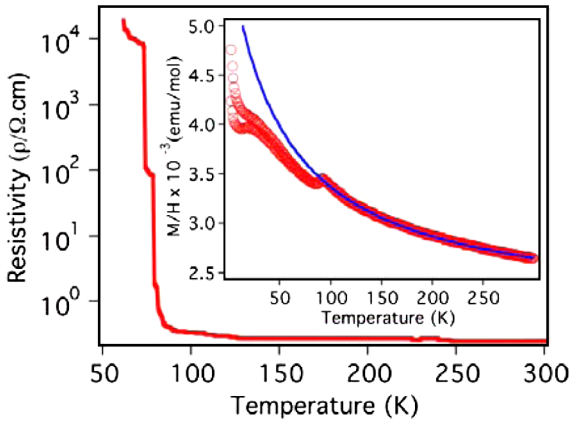

FIG. 2 (color online). Resistivity variation for $PbRuO_3$; the inset shows magnetic susceptibility measured in a 1 T field with a modified Curie-Weiss fit as described in the text.

magnitude (and was immeasurably large below 60 K), signifying a metal-insulator transition at $T_{MI} = 90$ K. This transition is also evident in magnetization data. The high temperature susceptibility is fitted as $\chi = C/(T - \theta) + \chi_p$, a sum of Curie-Weiss and Pauli paramagnetic terms, respectively, with $\chi_p = 2.09(1) \times 10^{-3}$ emu/mol, Curie constant $C = 0.195$ emu K/mol (corresponding to a paramagnetic moment of $1.25\mu_B$), and a Weiss temperature $\theta = -54$ K. Similar large temperature-independent contributions have been reported for nonperovskite ruthenates such as the pyrochlore $Tl_2Ru_2O_7$ ($\chi_p \approx 2 \times 10^{-3}$ emu/mol) [15] close to metal-insulator instabilities. A small dip is observed in the magnetic susceptibility on cooling through T_{MI}, showing that antiferromagnetic correlations are present in the insulating state. However, no long range magnetic transition is evident down to 4 K, although a broad hump with divergence between field- and zero-field-cooled susceptibilities is observed below 50 K.

A strong coupling of structure to the metal-insulator transition is observed in both x-ray and neutron powder diffraction measurements (Fig. 3). $PbRuO_3$ remains orthorhombic down to 1.5 K; however, the lattice parameters and volume change discontinuously on cooling through the transition (Fig. 4), and, surprisingly, the *Pnma* superstructure reflections with odd $(h + k + l)$ values disappear (see Fig. 3 inset). No new superstructure reflections, peak broadenings, or splittings were observed in the low temperature diffraction patterns of $PbRuO_3$, which are indexed by the body-centered space group *Imma*. This describes another common tilting superstructure of perovskites, and a refined *Imma* model gives excellent fits to both x-ray and neutron data [12]. Fits of lower-symmetry, acentric body-centered structures were unsuccessful. No magnetic diffraction peaks were observed down to 1.5 K in the GEM time-of-flight neutron diffraction data or in subsequent constant wavelength profiles collected from instrument E6 at the HZB reactor. We estimate the upper limit for any ordered Ru moment to be $\sim 0.5\mu_B$.

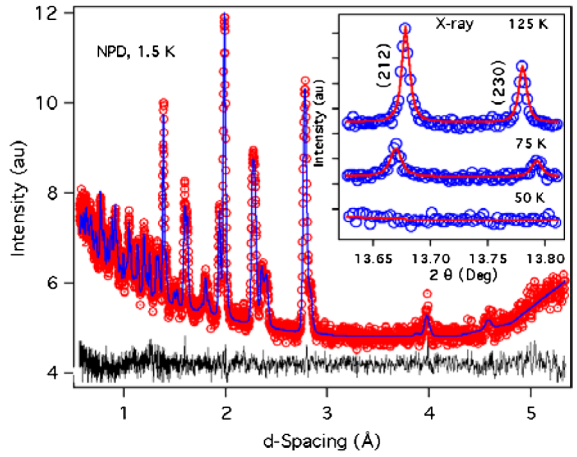

FIG. 3 (color online). Fit of the *Imma* model to the time-of-flight neutron diffraction profile of $PbRuO_3$ at 1.5 K. The inset shows the disappearance of *Pnma* x-ray superstructure reflections as the *Imma* phase is formed on cooling.

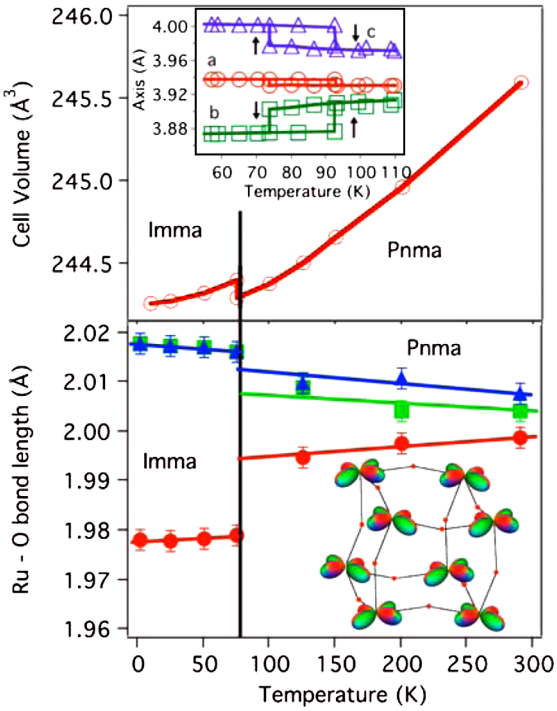

FIG. 4 (color online). Cell volume (top) and Ru-O distance (bottom) variations for $PbRuO_3$ from fits to neutron diffraction data. The upper inset shows hysteresis in the lattice parameters, normalized to the cubic perovskite cell, from x-ray measurements while warming or cooling at 10 K/min. Idealized d_{xy} orbital order in the *Imma* phase is shown in the lower panel.

The (high temperature) *Pnma* to (low temperature) *Imma* transition in $PbRuO_3$ is remarkable as *Pnma* is a subgroup of *Imma*, so a continuous group-subgroup transition from *Imma* to *Pnma* is allowed in Landau theory and is observed in many simple perovskites such as $SrSnO_3$ [16]. The *Pnma-Imma* "subgroup-group" transition in $PbRuO_3$ is clearly first-order, with a small volume anomaly typical of metal-insulator transitions and a substantial hysteresis of 20 K in the cell parameters between warming and cooling experiments (Fig. 4). The subgroup-group structural contribution to the transition entropy is negative, but this is evidently outweighed by the large positive electronic contribution from the delocalization of Ru 4*d* electrons.

The evolution of the Ru-O bond distances (Fig. 4) reveals an important aspect of the metal-insulator transition. At room temperature, the RuO_6 octahedra are almost regular with Ru-O bond lengths of 2.00–2.01 Å, but, below T_{MI}, a Jahn-Teller distortion is apparent in the *Imma* structure, with two short Ru-O1 bonds (1.97 Å) aligned approximately along z and four long Ru-O2 bonds (2.02 Å) in the xy plane. To a first approximation, this corresponds to a $d^2_{xy}d^1_{xz}d^1_{yz}$ orbital ordering of the $Ru^{4+}t^4_{2g}$ configuration in the insulating *Imma* phase, creating planes of minority-spin-occupied d_{xy} orbitals, as shown in Fig. 4. Pb^{2+} shows an unusual *A*-site distortion, having a near-regular square pyramidal coordination with five short Pb-O bonds (Pb-O1, 2.51 Å × 1; Pb-O2, 2.50 Å × 4), while other Pb-O distances are >2.82 Å. The O1-Ru-O2 angle of 122.5° shows that this is not a lone pair effect, for which an angle of <90° is expected. The Pb and Ru distortions are cooperative as O1 forms short bonds to Ru and only one short bond to Pb, whereas O2 has long bonds to Ru and four short bonds to Pb.

To clarify the orbitally ordered state, we have carried out LSDA + U calculations for the *Imma* phase with an effective Hubbard $U = 3.5$ eV [17]. Spin-orbit coupling (SOC) was also included since this ~160 meV interaction is large relative to the calculated crystal field splitting between the d_{xy} and d_{xz}/d_{yz} levels of ~50 meV. Our LSDA + U + SOC calculations gave an insulating ground state with a small gap of ~0.1 eV, verifying that $PbRuO_3$ is in the vicinity of a metal-insulator transition. The minority spin electron has a $0.46(1 + i)d_{xy} - 0.38(1 - i)(d_{xz} + d_{yz})$ orbital state which consists of 42% d_{xy}, 29% d_{xz}, and 29% d_{yz}, with d_{xy} being dominant as expected from the above structural results. Different magnetic solutions lie close in energy; e.g., the lowest *G*-type antiferromagnetic state is only 6.8 meV/f.u. below the ferromagnetic state, in keeping with the observed lack of magnetic order discussed below.

The insulating, orbitally ordered ground state of $PbRuO_3$ is anomalous in comparison to the other $ARuO_3$ perovskites (A = Ca, Sr, Ba), which remain metallic to the lowest temperature. This is not due to a size effect as $CaRuO_3$ has the most tilted *Pnma* superstructure but is stable to orbital order. (The combination of small Ca^{2+} and an imposed tetragonal symmetry in layered Ca_2RuO_4 is sufficient to induce a weak orbital order [18], but this phase is a Mott insulator.) The electronic nature of Pb is a key factor, and Ru 4*d*-Pb 6*s*6*p*-O 2*p* hybridizations are evident in the above band structure calculations. This Pb^{2+} covalency is sometimes manifest as a lone pair distortion resulting in ferroelectricity, e.g., in $PbTiO_3$, but lone pair distortions are not observed in either the *Pnma* or the

Imma phases of $PbRuO_3$. Another consequence of covalency is the stabilization of lower Pb^{2+} coordination numbers than expected from cation size arguments [19] as shown by the change from three short (2.47 Å) Pb-O bonds in the *Pnma* structure of $PbRuO_3$ to five, described above, in the *Imma* phase. The metal-insulator transition in $PbRuO_3$ is thus driven by electronic instabilities of both cations as the orbital order of $t_{2g}^4 Ru^{4+}$ is coupled to an order of s^2p^0 Pb^{2+} hybrid states. By contrast, Ru-orbital order is suppressed, and the metallic state remains stable in the other $ARuO_3$ perovskites that lack *A*-cation instabilities.

Orbital order lowers magnetic dimensionality relative to the structural dimensionality, and this can open a spin gap in some nonperovskite ruthenates, e.g., a singlet dimerized phase in $La_4Ru_2O_{10}$ [20,21] and possible Haldane chains in $Tl_2Ru_2O_7$ [15]. This seems not to be the case here; however, the observation of a broad susceptibility maximum at 25 K and the lack of a long range magnetic transition down to 1.5 K, which in conjunction with a Weiss temperature of −54 K corresponds to a frustration factor $|\theta/T_c| > 36$, shows that $PbRuO_3$ does not have a conventional ordered magnetic ground state. The divergence of field- and zero-field-cooled susceptibilities evidences some glassy character to the ground state, but there is no obvious source for structural disorder. One possibility is that the combination of orbital order and octahedral tilting (which gives a Ru-O-Ru angle of 159.8°) weakens nearest neighbor antiferromagnetic superexchange interactions in the *xy* plane so that they become comparable to the next nearest neighbor couplings. This frustrates spin order in the *xy* plane, leading to one-dimensional (*z* direction) magnetic behavior in the three-dimensional perovskite lattice imposed by orbital order.

In summary, the low temperature properties of $PbRuO_3$ show that normally hidden orbitally ordered states such as that of degenerate $t_{2g}^4 Ru^{4+}$ ions in ruthenate perovskites may be stabilized by coupling to electronic instabilities of other cations. This may provide a strategy for accessing orbitally ordered states of other 4*d* and 5*d* transition metal oxide networks. The combined order of Pb *s* and *p* hybridized orbitals, Ru *d* orbitals, and O-centered octahedral tilting instabilities results in an anomalously high symmetry ground state structure that inverts the usual group-subgroup symmetry descent. These distortions also suppress long range spin order in $PbRuO_3$, and further experiments and theoretical work will be needed to elucidate the magnetic ground state.

We acknowledge EPSRC for support and the provision of ESRF and ISIS beam time and the Leverhulme trust for additional support. H. W. and D. I. K. are supported by DFG through SFB 608. We thank J. W. G. Bos (Edinburgh), P. G. Radaelli (ISIS), and N. Stüer, A. Buchsteiner, and D. A. Tennant (HZB) for assistance with diffraction measurements and useful discussions.

*Corresponding author.
j.p.attfield@ed.ac.uk

[1] Y. Tokura, Rep. Prog. Phys. **69**, 797 (2006).
[2] K. Ishida *et al.*, Nature (London) **396**, 658 (1998).
[3] S. A. Grigera *et al.*, Science **294**, 329 (2001).
[4] J. M. Longo, P. M. Raccah, and J. B. Goodenough, J. Appl. Phys. **39**, 1327 (1968).
[5] D. J. Singh, J. Appl. Phys. **79**, 4818 (1996).
[6] I. I. Mazin and D. J. Singh, Phys. Rev. B **56**, 2556 (1997).
[7] C.-Q. Jin *et al.*, Proc. Natl. Acad. Sci. U.S.A. **105**, 7115 (2008).
[8] L. Klein *et al.*, Phys. Rev. B **60**, 1448 (1999).
[9] J. A. Kafalas and J. M. Longo, Mater. Res. Bull. **5**, 193 (1970).
[10] A. C. Larson and R. B. Von Dreele, Report No. LAUR 86-748, 1998.
[11] C. W. Jones, P. D. Battle, P. Lightfoot, and W. T. A. Harrison, Acta Crystallogr. Sect. C **45**, 365 (1989).
[12] Refined *x*, *y*, and *z* coordinates and isotropic *U* factors for neutron refinements of $PbRuO_3$ in space group *Pnma* at 290 K [and in *Imma* at 25 K where different]: Pb: 0.0120 (5) [0], 0.25, 0.9955(4) [0.9868(1)], and 0.0075(3) Å^2 [0.0001(1) Å^2]; Ru: 0, 0, 0.5, and 0.0026(3) Å^2 [0.0010(1) Å^2]; O1: 0.4991(1) [0.5], 0.25, 0.0638(5) [0.0705(2)], and 0.0077(5) Å^2 [0.0032(2) Å^2]; O2: 0.2745(4) [0.25], 0.0359(2) [0.0456(1)], 0.7255(4) [0.75], and 0.0088(4) Å^2 [0.0034(1) Å^2]. Cell parameters are shown in the abstract. Reduced chi-squared = 1.27 [1.77] and weighted profile residual $R_{wp} = 0.022$ [0.026].
[13] H. Kobayashi, M. Nagata, R. Kanno, and Y. Kawamoto, Mater. Res. Bull. **29**, 1271 (1994).
[14] P. Blaha, K. Schwarz, G. K. H. Madsen, D. Kvasnicka, and J. Luitz, WIEN2K code, http://www.wien2k.at. The muffin-tin sphere radii were 2.5, 2.1, and 1.5 Bohr for Pb(Sr), Ru, and O, respectively, the cutoff energy of the plane wave expansion was set at 16 Ryd, and 1600 *k* points were used for integration over the Brillouin zone. Structural relaxations gave lattice constants only 1.2% smaller than the experimental ones and atomic displacements ≤0.02 Å.
[15] S. Lee *et al.*, Nature Mater. **5**, 471 (2006).
[16] E. H. Mountstevens, S. A. T. Redfern, and J. P. Attfield, Phys. Rev. B **71**, 220102(R) (2005).
[17] *U* was calculated following G. K. H. Madsen and P. Novák, Europhys. Lett. **69**, 777 (2005).
[18] I. Zegkinoglou, Phys. Rev. Lett. **95**, 136401 (2005).
[19] Hence a high pressure is needed to increase the Pb oxygen coordination from 8 in the ideal pyrochlore structure of $PbRuO_{3(+x)}$ to 12 in the ideal perovskite arrangement, while $SrRuO_3$ is thermodynamically stable at ambient pressure. This effect is also evident in the room temperature *Pnma* perovskite structures. The lattice parameters of $PbRuO_3$ are slightly larger than those for $SrRuO_3$ ($a = 5.535$, $b = 7.851$, $c = 5.572$ Å), but the three short (<2.6 Å) Pb-O distances in $PbRuO_3$ (2.47 Å × 3) are shorter than the corresponding Sr-O distances in $SrRuO_3$ (2.51 × 1 and 2.52 × 2 Å).
[20] P. Khalifah *et al.*, Science **297**, 2237 (2002).
[21] H. Wu *et al.*, Phys. Rev. Lett. **96**, 256402 (2006).